Optical Examination of Shockwave Propagation Induced by an Underwater Wire Explosion

O Higa[1,2]*, A Yasuda[2], Y Higa[1], K Shimojima[1], K Hokamoto[2], S Itoh[1]

1. National Institute of Technology, Okinawa College, Japan
2. Kumamoto University, Japan

ABSTRACT

We have been investigating underwater-explosion-induced shockwave-propagation phenomena for use in a robust food-processing system. This system comprises a high-voltage capacitor bank with a gap switch, water tank, and wire explosive. We performed an optical examination of the shockwave generated by a wire explosion using an electrical discharge in the water tank. Simultaneously, we measured the shock pressure and investigated the effects of various electrical characteristics upon the shockwave propagation phenomena. To obtain various strengths of the underwater shockwave, 0.6-, 1.0-, and 1.4-mm width wires made from 1.0-mm-thick aluminum plates were used at various voltages. As an example, a shockwave with a propagation velocity of 1,600 m/s was observed from an explosion generated using a 1.0-mm-width aluminum wire. We found that the strength of the shockwave could be controlled by the applied discharge voltage and wire size.

1. INTRODUCTION

We have been developing food-processing devices using underwater shockwaves generated by electrical discharges [1-10]. Figure 1 is a rice powder-manufacturing system [11-13]. The rice powder-manufacturing system mills rice by applying a shockwave to the rice that circulates in a silicone tube placed in the pressure vessel. This device presently employ shockwaves generated in water using a gap discharge technique. However, we propose to employ a wire-explosion technique instead, as it is capable of generating higher-pressure shockwaves. To this end, we need to estimate the wire-explosion-induced shockwave characteristics in the device. Therefore, in this study, we aim to accomplish this goal through optical observation and pressure measurements.

2. EXPERIMENTAL

2.1 EXPERIMENTAL SETUP

Figure 2 shows the device used in the present experiment, which employed the wire-explosion method. A thin metal wire is set between two electrodes in water. When pulse power is applied to the wire, the electrical energy rapidly sublimates the wire, thus

*Corresponding Author: osamu@okinawa-ct.ac.jp

converting it into plasma along with the surrounding water. At this instant, an underwater shockwave is generated around the rapidly expanding plasma [11] [14-16]. A high-voltage pulse generator is used for supplying high-voltage, large-current electrical discharge to the wire (Figure 2A). The device can be charged and discharged at a frequency of 10 shots/min, an energy of 4.9 kJ, and a charging voltage of 3.5 kV. The device is equipped with a fixing jig for holding the discharge electrodes along with the electrode wire (Figure 2B). An aluminum wire with a thickness of 1 mm and a length of 3 mm was used for the blasting section, and the widths used were 0.6, 1.0, and 1.4 mm.

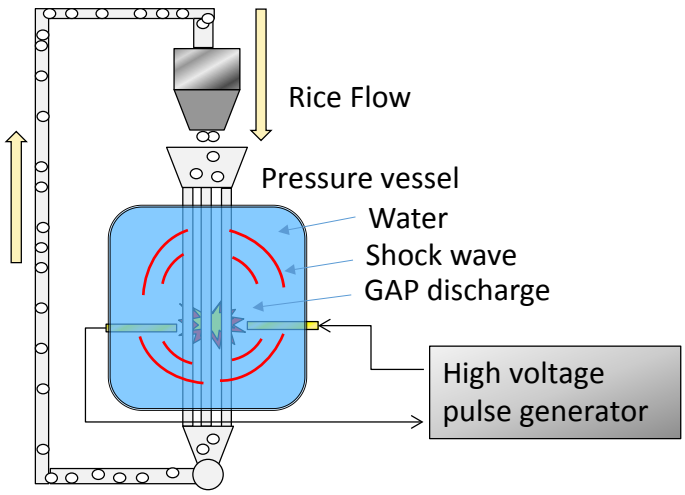

Figure 1: Rice powder manufacturing system using underwater shockwaves

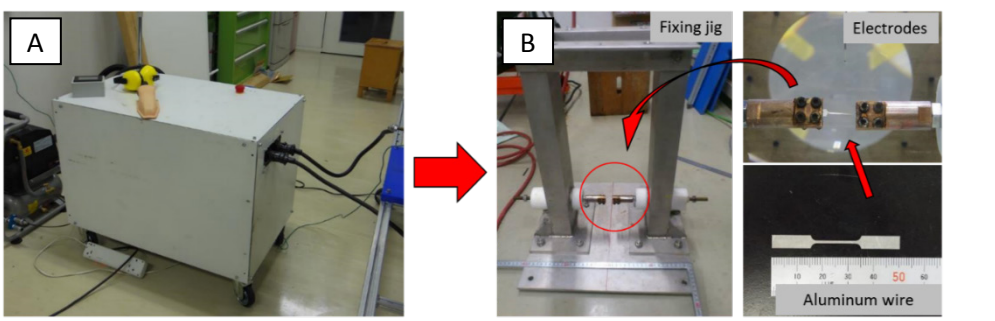

Figure 2: High-voltage pulse generator and the fixing jig holding the electrodes.

The images of the underwater shockwave were acquired using the Schlieren method. Figures 3 and 4 show a schematic of the experimental setup used for Schlieren photography. The experimental apparatus included a single wavelength pulse laser, condenser lens, pinhole, and knife-edge. A fixed jig that is set to the vessel has two windows for visualization, one each in the front and the back. The pulse laser emission is synchronized

with the wire explosion and the change in the water density caused by the propagation of the shockwave that is visualized by a change in the refractive index, thereby enabling this propagation to be optically captured using a high-speed camera (Specialised Imaging, Kirana-5M).

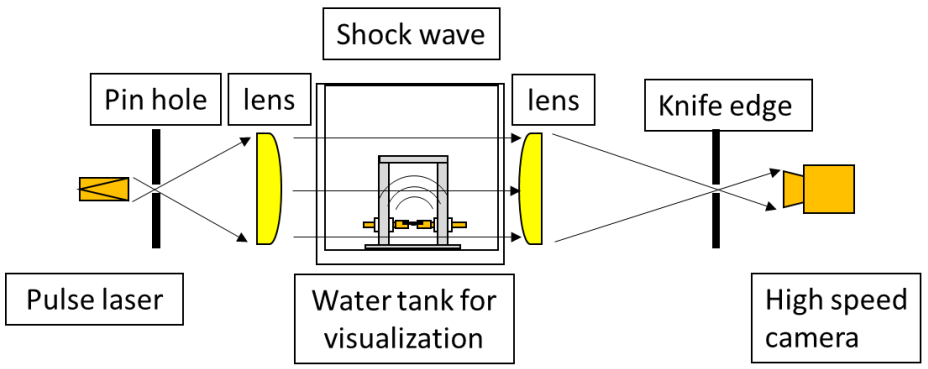

Figure 3: Construction of the optical system based on the Schlieren method.

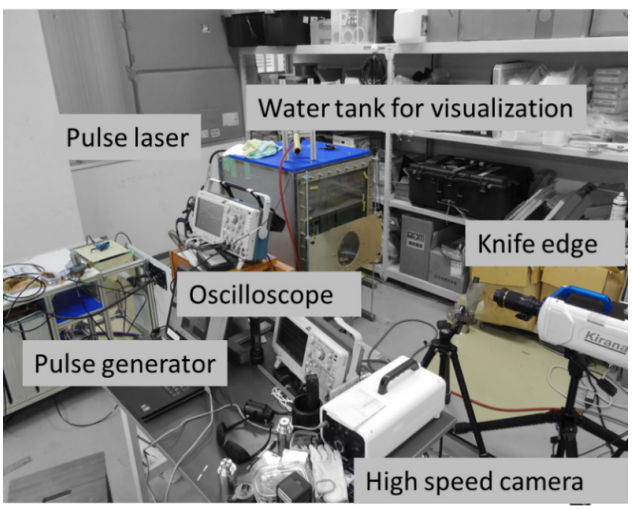

Figure 4: Experimental setup used for optical observation

Figure 5 shows the details of the pressure sensor setup that was used concurrently with the optical observation. A pressure sensor procured from Müller Instruments (Müller-Platte Needle Probe, 100-100-1, rise time 30 ns) was installed 30 mm above the aluminum wire. The pressure sensor is installed to insulate the jig by removing noise at the time of discharge. Signals from the pressure sensor were measured using a digital storage oscilloscope (Tektronix MDO3024, 200 MHz, 2.5 GS/s). In addition, the discharge voltage and current were measured using a high-voltage probe (TES TEC, HVP-15HF, MAX. 10 kV rms, 50 MHz) and a current probe (CWT, 1500B mini, 0.02 mV/A), respectively. Both the oscilloscope and the high-speed camera were triggered by the signal from the current probe.

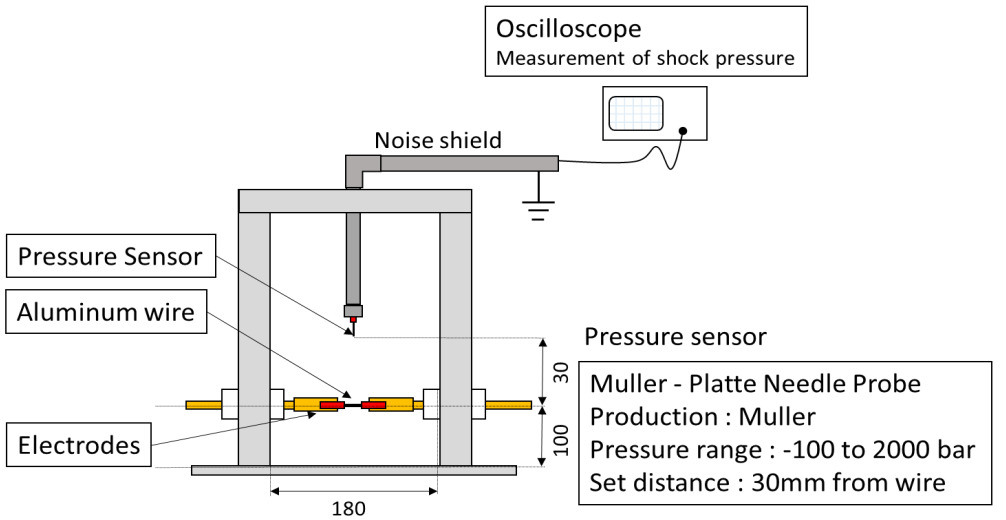

Figure 5: Installation details of the wire and the pressure sensor.

2.2 EXPERIMENTAL METHODS

We evaluated the underwater shockwave generated by each of the wires using the following procedure. First, we measured the shock pressure at a point 30 mm above the wire and the electrical characteristics at the time of discharge. Simultaneously, the propagation of the underwater shockwave was visualized. Then, the propagation distance was plotted as a function of elapsed time after the wire explosion. The propagation velocity at each propagation distance was calculated using the nonlinear curve-fitting method. Further information on the shock pressure of the water was calculated from the propagation velocity using Hugoniot data. Finally, the shock pressure was evaluated using the discharge characteristics of each wire.

3. RESULTS AND DISCUSSION

The voltage–current characteristics and waveform of the pressure sensor (purple line) are shown figure 6 for the case in which the wire used is of 1 mm width, 1 mm thickness, and 3 mm lengthand is exploded with a charging voltage of 3.5 kV. The gap voltage (blue line) was calculated from the difference between the two electrode voltages. The power (green line) and the discharge energy (yellow line) were calculated from the gap voltage and discharge current (red line), respectively. The discharge voltage was applied to the electrode 36 μs before triggering, and the discharge current rose simultaneously. The gap voltage decreased with the energy consumed by the wire. When the wire explosion began 29.8 μs after the trigger, the gap voltage increased along with the resistance between the electrodes. The energy applied to the wire was 1.57 kJ. The shockwave generated by the wire explosion reached the pressure sensor located 30 mm above the wire 49 μs after triggering. The shock pressure caused by the shockwave was 17.3 MPa at the sensor position. In addition, the detonation time of the wire was 6.9 μs. A representative image of the underwater shockwave, acquired using the Schlieren method, is shown in Figure 7. The image was

acquired at a frame rate of 1 Mf/s, exposure time of 1 µs, and flash time of 10 ns. The high-speed camera was triggered by an input from the oscilloscope. The wire explosion began 28 µs after the trigger, and the shockwave reached the pressure sensor simultaneously as the electrical measurement. Figure 8 shows the characteristics of the propagation distance as a function of the propagation time in case of the wire with a width of 1 mm. The data in the plot are measurement values determined from optical observations. The fitting curve was calculated approximately from the plot data using equation (1) [14].

$$\begin{aligned} X \;=\; & A_1\,[\,1 \,-\, e^{\,-B_1\,T}\,] \\ & +\,A_2\,[\,1 \,-\, e^{\,-B_2\,T}\,] \\ & +\,A_3\,[\,1 - e^{\,-B_3\,T}\,] \,+\, C_0\,T \end{aligned} \tag{1}$$

X: Propagation distance, T: Time from explosion, C_0: Underwater Sonic velocity A_1, B_1, A_2, B_2, A_3, B_3: Fitting parameters

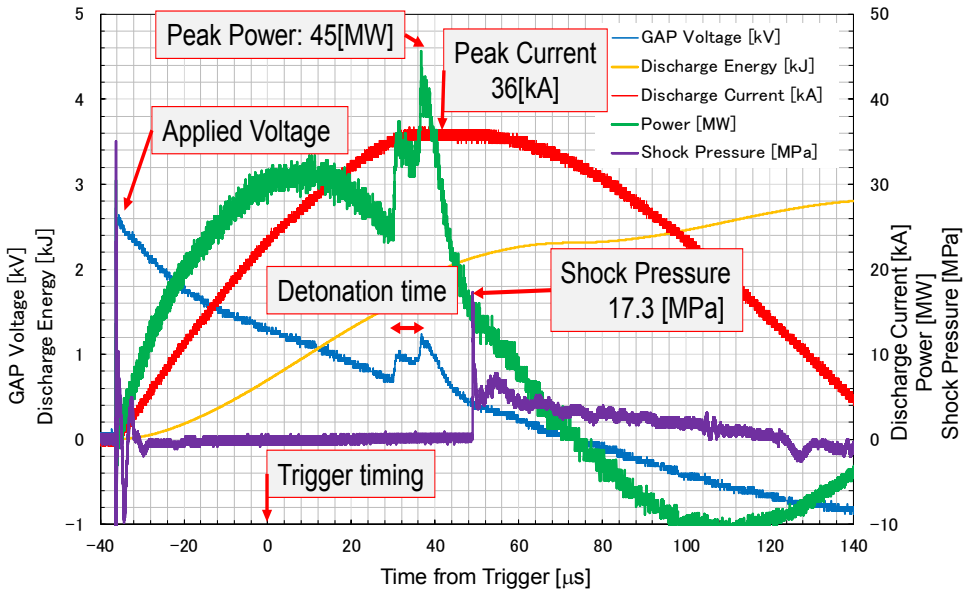

Figure 6: Voltage–current characteristics and waveform of pressure sensor on a 1 mm wire.

Figure 9 shows propagation velocity and shockwave pressure as a function of the propagation distance. The horizontal axis shows propagation distance from the wire. The left vertical axis shows the propagation velocity of the shockwave and the right axis shows the shockwave pressure. The propagation velocity and the shockwave pressure were calculated on the basis of the fitting curve using Hugoniot data and Equation (2) [17-19]. The propagation velocity decreased with distance and achieved sonic velocity at a distance of 70 mm. The shockwave pressure calculated was 132 MPa near the wire and decreases to 20 MPa at a distance of 30 mm. This result is in agreement with the value measured by the pressure sensor.

$$P = P_0 + \rho U_s \frac{(U_s - C_0)}{S} \quad (2)$$

C_0: Underwater Sonic velocity (1503 [m/s]), S: Linear Hugoniot slope coefficient (1.79), P: Shock Pressure [MPa], P_0: Initial Pressure (0.1 [MPa]), ρ: Density of water (1000 [kg/m^3]), U_s: Shock velocity [m/s],

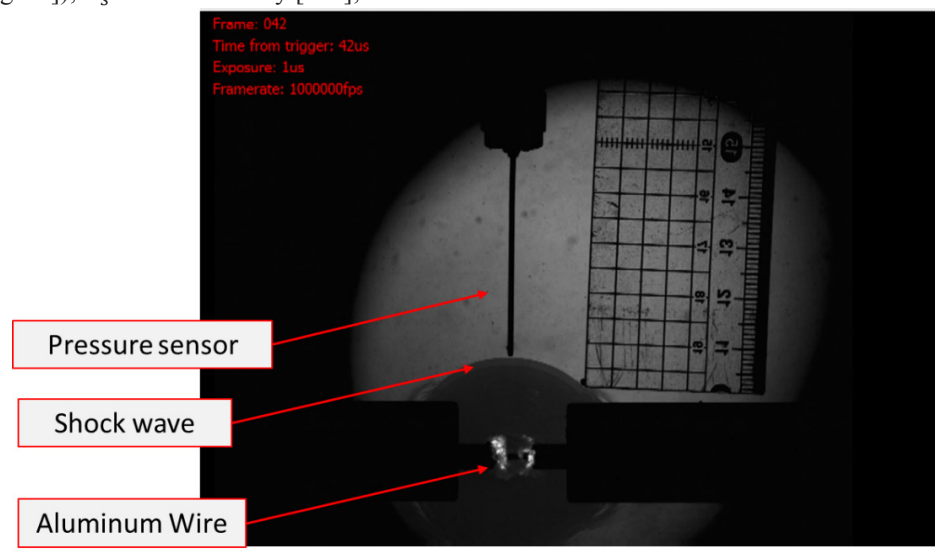

Figure 7: The visualization photograph of underwater shockwave taken by schlieren method.

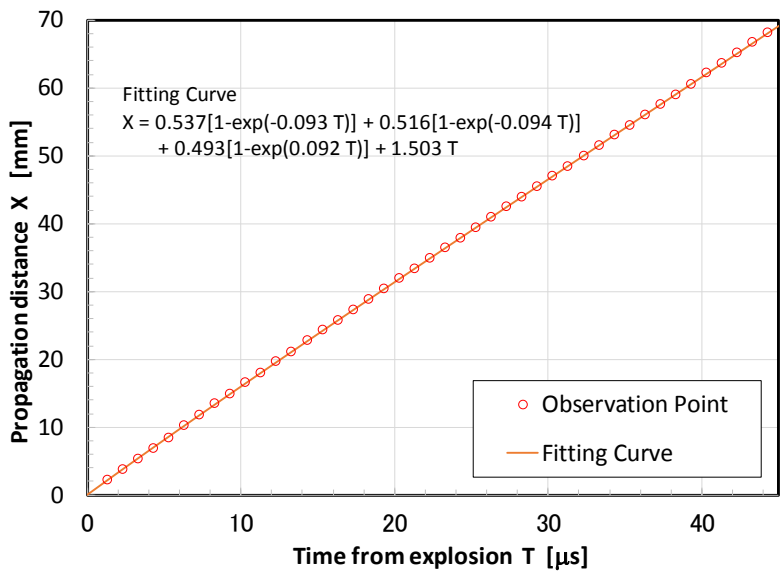

Figure 8: Propagation distance depending on the propagation time for a 1 mm width wire

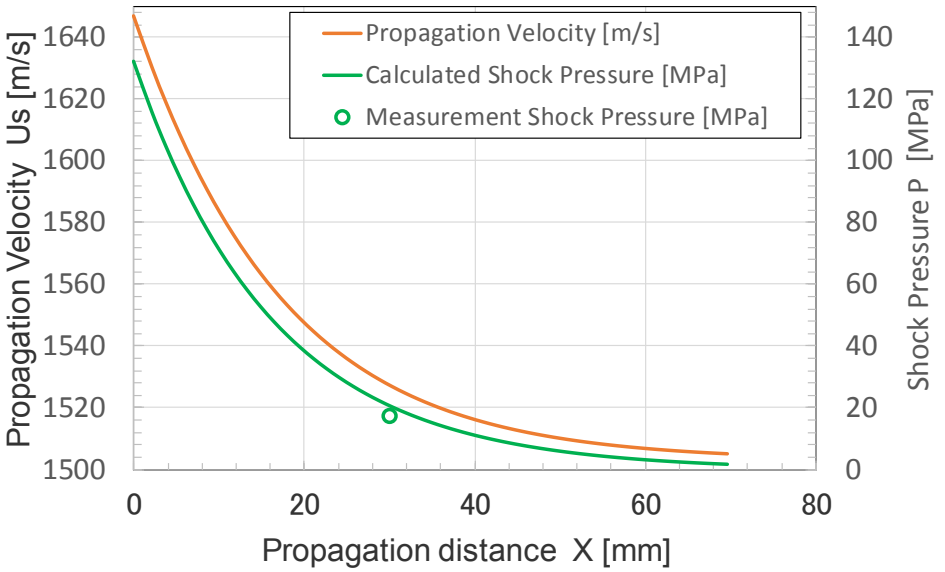

Figure 9: Propagation velocity and shock pressure depending on propagation distance for a 1 mm wire.

The shockwave pressures that occur with various wires were evaluated to optimize the construction of our system. Figure 10 shows the relationship between propagation distance and pressure of the shockwaves generated using three types of wires. The blue line shows the pressure of the shockwave due to a 0.6-mm width wire, the green line shows the result for a 1-mm width wire, and the red line shows the result for a 1.4 mm wire. In Figure 10, these lines were calculated on the basis of the fitting curve using Hugoniot data and Equation (2) as same as Figure 9. Furthermore, the points of the same color correspond to values measured by the pressure sensor.

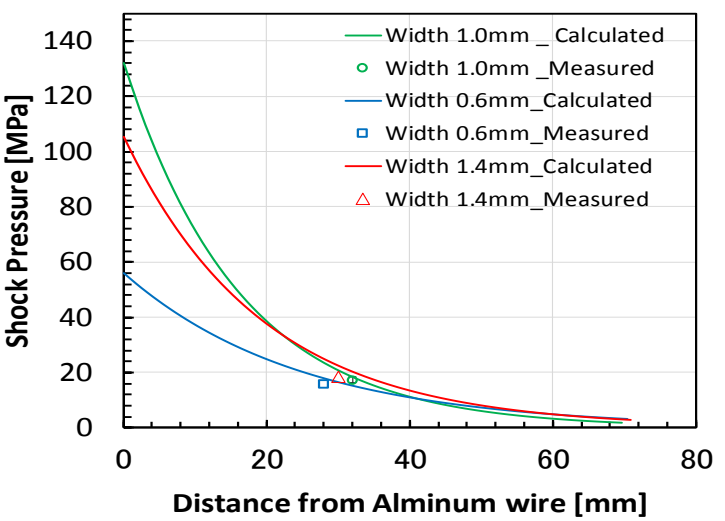

Figure 10: Shock pressure dependence on the distance from the aluminum wire.

Figure 11 shows the shock pressure at a propagation distance of 30 mm for each width of the wire. Data shows the average of measure from the pressure sensor. The results indicate that the pressure of a shockwave caused by a wire explosion is dependent on the size of the wire. The shockwave had the highest pressure (132 MPa) near the 1-mm width wire. Conversely, the shockwave pressure was the lowest in the case of a 0.6-mm width wire (56 MPa). Although a great difference between the shockwave pressures was not observed at a propagation distance of 30 mm, the pressure from the 1-mm width wire was still the highest. The measured values from a 1-mm width wire had a smaller dispersion. When the 0.6- or Figure 12 shows the results for wire of widths 0.6, 1.0, and 1.4-mm and at a distance of 30 mm. The horizontal axis show the lapsed time from the triggering at the time of the electrical discharge, and the left and right axes are the voltage between the electrodes/electric discharge energy and the pressure value of the shockwave, respectively.The blue line indicates the voltage between the electrodes, the black line indicates the electric discharge energy injected into the electrodes, and the purple line indicates the waveform recorded by the pressure sensor. It can be seen from the figure that there are some regions where the waveform is disturbed. These correspond to the explosion of the wire. It is observed that the time to explosion changes with the width of the wire, and the difference also appears in the injection energy. Moreover, it turns out that detonation time also changes with the width of the wire. Figure 13 shows the relationship between the initial shock pressure and "$\frac{E_{exp}}{\Delta T_{exp}}$" It is evident that the initial shock pressure increases depending on the value of "$\frac{E_{exp}}{\Delta T_{exp}}$" This result shows that the shock pressure is the highest when a 1-mm width wire is used.

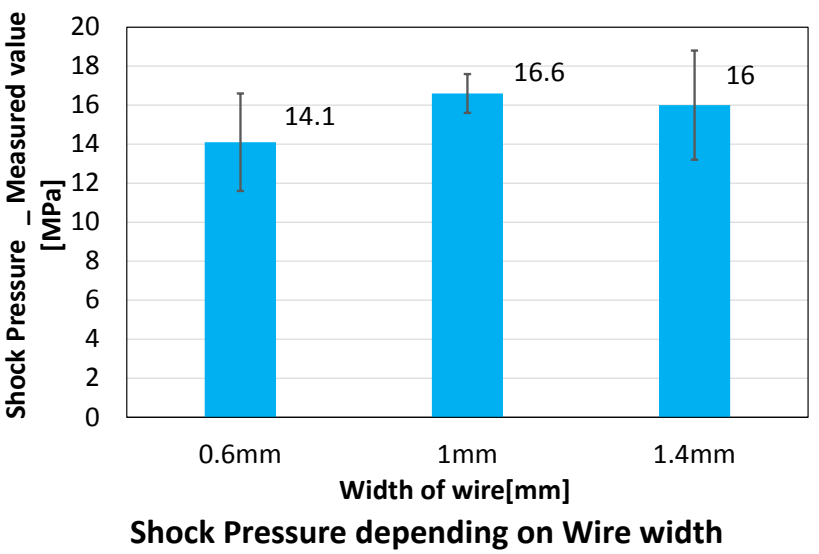

Figure 11: Shock pressure depend on wire width at 30mm from the wire.

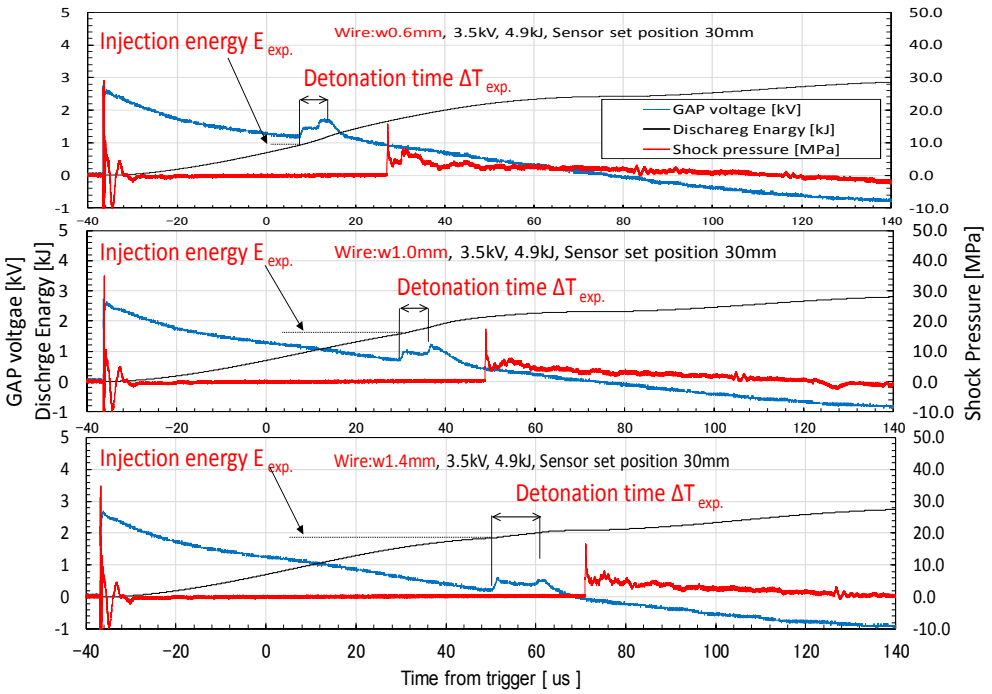

Figure 12: Electric characteristics depending on the wire width.

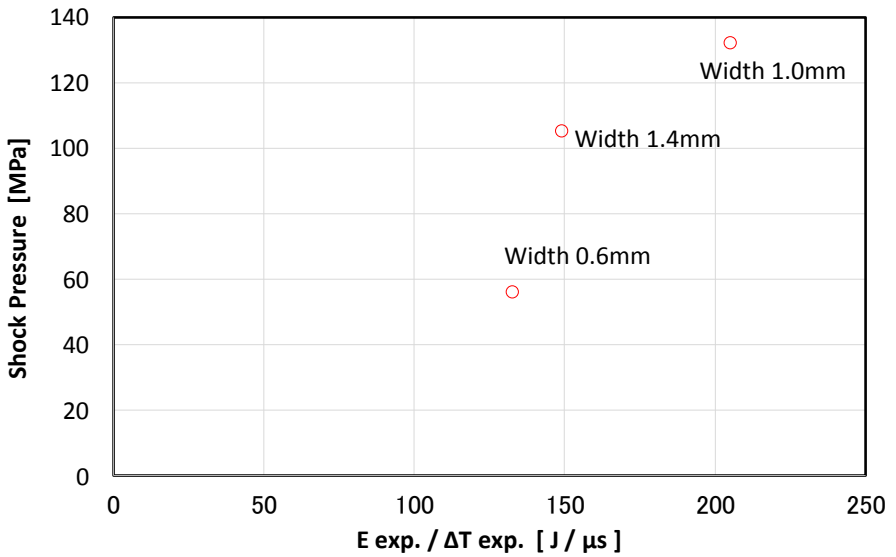

Figure 13: Relationship between discharge characteristics ($\frac{E_{exp}}{\Delta T_{exp}}$) and shock pressure.

4. CONCLUSION

We optically observed the shockwave generated from a wire explosion in water and calculated the pressure specific to this shockwave using the approximate propagation characteristic function and the curve-fitting method for a shockwave. The calculated propagation specificity of the shockwave is in agreement with the value measured by a pressure sensor at a propagation distance of 30 mm. We evaluated the variation in the shock pressure as a function of the width of the wire and demonstrated that shock pressure is also associated with the electric discharge specific to the wire explosion. We reasoned that the most appropriate wire width is 1 mm, because it causes the largest shockwave pressure at the highest "$\frac{E_{exp}}{\Delta T_{exp}}$".

ACKNOWLEDGEMENT

This study was supported by Ministry of Agriculture, Forestry and Fisheries and JSPS KAKENHI Grant Number 15H00339.

REFERENCES:

[1] K. Higa, T. Matsui, S. Hanashiro, O. Higa, S. Itoh, Evaluation of the contact switch materials in high voltage power supply for generate of underwater shockwave by electrical discharge, *The International Journal of Multiphysics*, Vol.8, No.4, 2015.

[2] O. Higa, K. Higa, H. Maehara, S. Tanaka, K. Shimojima, A. Takemoto, K. Hokamoto, S. Itoh, Effects of Improving Current Characteristics of Spark Discharge on Underwater Shock waves, *The International Journal of Multiphysics*, Vol.8, No.2, pp.245-252, June 2014.

[3] O. Higa, T. Matsui, R. Matsubara, K. Higa, S. Itoh, Improvement effect of Discharge Circuit for the Underwater Shock Wave, *Materials Science Forum* , Vol.767, pp199-204, 2014.

[4] Y. Seki, H. Fukuoka, Y. Miyafuji, H. Iyama, O. Higa, S. Itoh, Study on Behavior of Underwater Shock Wave in Enclosed Vessel, *Materials Science Forum*, Vol.767, pp68-73, 2014.

[5] T. Matsui, K. Higa, R. Matsubara, S. Hanashiro, O. Higa, S. Itoh, Measurement of Discharged Energy and Pressure of Underwater Shockwave Changing Materials of Contact Switch in High Voltage Power Supply, *Materials Science Forum*, Vol 767, pp.250-255, 2014.

[6] S. Hanashiro, K. Higa, T. Matsui, R. Matsubara, O. Higa, S. Itoh, Development of a power supply for the food processing device, using high pressure due to evaporation of aluminium wire by discharging high current, *Materials Science Forum*, Vol.767, pp244-249, 2014.

[7] Y. Omine, T. Gushi, O. Higa, S. Itoh, Development and Improvement of the Experimental Apparatus using the Underwater Shock Wave, *Materials Science Forum*, Vol.767, pp256-260, 2014

[8] J. Marousek, S. Itoh, O. Higa, Y. Kondo, M. Ueno, R. Suwa, J. Tominaga, Y. Kawamitsu, Enzymatic hydrolysis enhanced by pressure shockwaves opening new possibilities in Jatropha Curcas L. processing, *Journal of Chemical Technology and Biotechnology*, Volume 88, Issue 9, pp1650-1653, September 2013

[9] J. Marousek, S. Itoh, O. Higa, Y. Kondo, M. Ueno, R. Suwa, J. Tominaga, Y. Kawamitsu, Pressure shock wave to enhance oil extraction from jatropha curcas l., *Biotechnology & Biotechnological Equipment*, Volume 27, Number 2, pp3654-3658, April 2013

[10] J. Marousek, S. Itoh, O. Higa, Y. Kondo, M. Ueno, R. Suwa, Y. Komiya, J. Tominaga, Y. Kawamitsu, The use of underwater high-voltage discharges to improve the efficiency of Jatropha curcas L. biodiesel production, *Biotechnology and Applied Biochemistry*, Volume 59, Issue 6, pages 451-456, November-December 2012

[11] O. Higa, R. Matsubara, K. Higa, Y. Miyafuji, T. Gushi, Y. Omine, K. Naha, K. Shimojima, H. Fukuoka, H. Maehara, S. Tanaka, T. Matsui, S. Itoh, Mechanism of the Shock Wave Generation and Energy Efficiency by Underwater Discharge, *The International Journal of Multiphysics*, 2012, Vol.6 No.2 pp.89-98.

[12] K. Shimojima, O. Higa, K. Higa, Y. Higa, A. Takemoto, A. Yasuda, M. Yamato, M. Nakazawa, H. Iyama, T. Watanabe, S. Itoh, Development of Milling Flour Machine of Rice Powder Using Instantaneous High Pressure, 1st Report, Development of Continuous Driving Device and Componential Analysis of Rice Powder, *Japan Journal of Food Engineering*, Vol.16 No. 4, 297-302, 2015-12

[13] K. Shimojima, Y. Miyafuji, K. Naha, O. Higa, R. Matsubara, K. Higa, Y. Higa, T. Matsui, A. Takemoto, S. Tanaka, H. Maehara, S. Itoh, Development of the rice-powder manufacturing system using underwater shock wave, *The International Journal of Multiphysics*, 2012, Vol.6 No.4 pp.355-364.

[14] M. Otsuka, Ph.D dissertation, 2007, Kumamoto University

[15] S. I. Tkachenko, D. V. Barishpoltsev, G. V. Ivanenkov, V. M. Romanova, A. E. Ter-Oganesyan, A. R. Mingaleev, T. A. Shelkovenko, S. A. Pikuz, Different mechanisms of shock wave generation and scenarios of second breakdown development upon electrical explosion of wires, *16th IEEE International Pulsed Power Conference (Volume:1)*, 2007, pp.877 – 880

[16] V. I. Lisitsyn, T. Muraki, H. Akiyama, Characterization of a shock wave generated by a wire explosion in water, *Journal of the Acoustical Society of Japan (E)* 18(2), 89-91, 1997.

[17] S. P. Marsh, LASL *Shock Hugoniot Data*, University of California Press, 1980

[18] R. S. Bradly, *High Pressure Physics and Chemistry*, Academic Press, 1963, Vol. 1

[19] R. Kinslow, *High-Velocity Impact Phenomena*, Academic, 1970, New York